



# Fluidization behaviour of various titania feedstocks

by S. Moodley \*, A. Kale<sup>†</sup>, D. Bessinger\*, C. Kucukkaragoz<sup>‡</sup> and R.H. Eric<sup>‡</sup>

## Synopsis

In the chloride process for TiO<sub>2</sub> pigment production, various titania feedstocks (i.e. rutile, synthetic rutile, slag, and upgraded titania slag (UGS)) are chlorinated in a fluidized bed reactor with petroleum coke at temperatures between 1000°C and 1100°C to yield gaseous metal chlorides. Although feedstock preference is largely based on TiO<sub>2</sub> content, feedstock physical properties (i.e. density, sphericity, size distribution, and porosity) differ; these differences will affect fluidization behaviour and can inadvertently affect conversion efficiency. For example, a high carryover from the reactor reduces particle residence time and decreases conversion rates. Owing to dwindling rutile reserves in the world, most chloride producers are forced to feed blends of feedstocks to their chlorinators; and so it becomes important to understand whether blends have an effect on the hydrodynamic properties of the bed.

This paper describes the physical characterization of different feeds and the determination of the elutriation constants for slag, rutile, synthetic rutile, and a blend (i.e. 50 wt% rutile, 50 wt% slag). A common feature of the tests was that particles finer than 75 µm tended more than any other size to be elutriated. The tested rutile, classified as a Geldart Group B material, had the lowest carryover, whereas the slags had the highest. Interestingly, the elutriation constant ( $k_i$ ) of the blend is lower than those of either of its individual components.

## Keywords

fluidization, elutriation, titania feedstocks, blowover, chlorination, hydrodynamics.

## Background

Titanium dioxide is used mainly as pigment for paints, plastics, paper, cosmetics, toothpaste, and inks. TiO<sub>2</sub> pigment is valued because it imparts whiteness, brightness, and opacity to materials. Two processing routes exist for the production of TiO<sub>2</sub> pigments. One is sulphate-based and the other chloride-based.

Fluidized bed technology is employed for the chlorination process, therefore physical characteristics such as density, size, and shape factor of the feedstock are important. The feedstock has to consist of particles of sufficient size and density in order for it to fluidize with minimal blowover from the chlorinator. Feed to chlorinators includes a

number of titania feedstocks – namely, synthetic rutile (SR), natural rutile, upgraded titania slag (UGS), high-grade slag, and titania slag produced from the smelting of ilmenite. Natural rutile is the preferred feedstock for chlorination, but owing to dwindling reserves other titania products are substituted as feed. The physical properties and phase chemistry of the feedstocks differ, which has an impact on the way in which each feedstock reacts in the chlorinator, even though the TiO<sub>2</sub> content might be similar.

Entrainment, carryover, and elutriation are terms that will be used throughout the paper, and are defined here. In vessels containing fluidized solids, the gas leaving carries some suspended solids; the flux of solids is called entrainment or carryover<sup>1</sup>. Elutriation refers to the selective removal of particles of individual sizes from the fluidized bed.

In bubbling fluidized-bed reactors, solids are thrown into the freeboard in one of three ways: (1) from the roof of a bursting bubble, (2) from the bubble wake, and (3) from the wake of a trailing bubble just as it coalesces with its leading bubble<sup>1</sup>. A high elutriation rate translates to a shorter residence for particles in the fluidized bed, which in turn adversely affects conversion efficiencies.

Carryover of a particular size fraction can be quantified by means of a measure called the elutriation constant ( $k_i$ ). Kunii and Levenspiel<sup>1</sup> describe a procedure for determining elutriation constants by means of batch experiments. Assuming that the flux rate of any particular size of solid  $i$  is proportional

\* Exxaro Resources, Pretoria, South Africa.

† Mintek, Johannesburg, South Africa.

‡ University of the Witwatersrand, Johannesburg, South Africa.

© The Southern African Institute of Mining and Metallurgy, 2012. SA ISSN 0038-223X/3.00 + 0.00. This paper was first presented at the, Industrial Fluidization South Africa Conference, 16–17 November 2011, Cradle of Humankind, South Africa.

## Fluidization behaviour of various titania feedstocks

to its weight fraction ( $x_i$ ) in the bed, all other factors being constant, the flux of particles out of the fluidized bed may be written as

$$-\frac{1}{A} \frac{dW_i}{dt} = k_i^* x_i = k \left( \frac{W_i}{W} \right) \quad [1]$$

If the total mass of the sample does not change much during a trial (i.e., < 20%), then integration of Equation [1] gives

$$\frac{W_i}{W_{i0}} = \exp\left(-\frac{k_i^* A t}{W}\right) \quad [2]$$

The elutriation constant can be calculated by Equation [2].

This paper examines the elutriation behavior of six samples—a rutile concentrate, SR, three different slags, and a blend of slag and rutile.

### Experimental details

#### Samples

The test samples included three titania slags from different producers (two from South Africa and a third from outside South Africa – Slag B), rutile, and SR.

#### Elutriation testwork

The elutriation tests were conducted in an externally heated quartz reactor. The quartz reactor was connected to a crossover duct, with the solids in the off-gas discharged through a cyclone and two collection flasks. The crossover duct provides a passage for the gas and elutriated particles to leave the silica reactor. A porous distributor plate divided the quartz reactor into two sections and allowed for the passage of gases for fluidization of the sample. The diameter of the lower section of the quartz reactor was 80 mm, and the height 300 mm. The diameter of the extended freeboard section was 110 mm, and the height 500 mm.

Each sample (600 g) was fluidized with nitrogen. The gas flow was maintained constant throughout the trial. Electrical power was used to raise the temperature of the fluidizing material to 1000°C; the heat-up period was 80 minutes. Each test ran with the bed fluidized for 30 minutes at 1000°C with a superficial gas velocity of 0.19 m/s. In the extended freeboard section of the reactor, the superficial gas velocity reduced to 0.10 m/s.

Gas exited at the top of the reactor and carried with it a fraction of the finer and lighter material. The elutriated solids were separated from the gas in the cyclone. The solids settled out in the round-bottom flask, while the gas passed through the off-gas duct and was vented from the system. After 30 minutes of fluidization at 1000°C, the power was switched off and the material cooled by the fluidizing gas. Upon conclusion of a fluidization test, the bed sample and carryover were collected, weighed, and the particle size distribution (PSD) measured.

### Results and discussion

#### Sample characterization

Chemical composition of the feedstock is reported in Table I.

The blend consists of a 1:1 ratio of Slag A and rutile. The particle size distribution and density are given in Table II. The chemical analysis was determined by inductively coupled plasma optical emission spectrometry (ICP – OES) techniques, and particle size by screening.

As a product of milling, the slags are angular and have a wider particle size distribution than natural rutile. Rutile particles are smoother and more spherical than the slag particles. The differences in the shape and size are evident from the scanning electron microscope (SEM) backscattered electron images shown in Figures 2 and 3.

#### Material properties

Geldart<sup>2</sup> proposed a classification of the fluidization behaviour of a bed of solid particles fluidized by air under normal ambient conditions. Beds of particles fall into one of four groups based on density and mean particle size, that is, Group A, Aeratable; Group B, Sandlike bubbling; Group C, Cohesive; and Group D, Spoutable (see Figure 4).

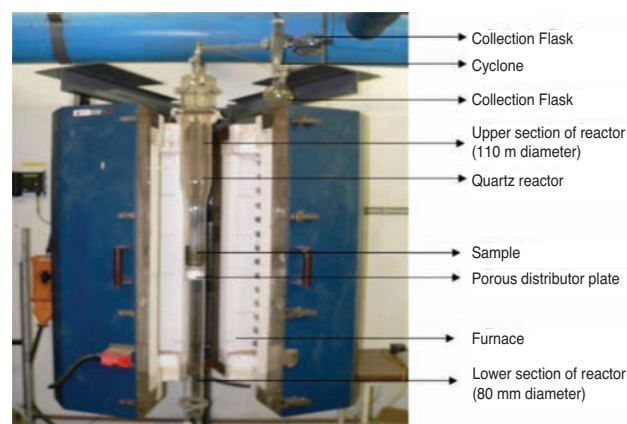


Figure 1—Photograph of the test apparatus

Table I

**Feedstock chemical analysis**

	Slag A	Slag B	Slag C	Rutile	SR	Blend
	(wt %)					
SiO <sub>2</sub>	1.64	1.49	1.83	1.44	0.80	1.36
Al <sub>2</sub> O <sub>3</sub>	1.02	1.64	1.23	0.31	1.80	0.78
FeO	8.60	1.96	11.00	0.49	3.43	4.52
Fe (metallic)	0.00	1.03	0.00	0.00	0.10	0.00
TiO <sub>2</sub> (equivalent)*	87.46	95.02	84.80	95.69	92.77	91.55
Ti <sub>2</sub> O <sub>3</sub>	23.42	38.80	24.30	0.00	10.30	9.99
TiO <sub>2</sub>	61.92	51.90	57.70	95.69	81.40	80.45
CaO	0.22	0.26	0.13	0.08	0.098	0.15
MgO	0.73	0.25	1.11	0.01	0.31	0.34
Na <sub>2</sub> O	0.02	0.03	0.01	0.00	0.01	0.00
K <sub>2</sub> O	0.03	0.01	0.03	0.00	0.00	0.00
MnO	1.90	2.80	1.72	0.01	1.00	1.03
P <sub>2</sub> O <sub>5</sub>	0.18	0.10	0.00	0.00	0.00	0.00
ZrO <sub>2</sub>	0.17	0.16	0.16	0.92	0.05	0.55
Nb <sub>2</sub> O <sub>5</sub>	0.16	0.08	0.11	0.00	0.23	0.00
Cr <sub>2</sub> O <sub>3</sub>	0.09	0.14	0.17	0.11	0.15	0.06
V <sub>2</sub> O <sub>5</sub>	0.46	0.21	0.46	0.49	0.32	0.29

\* Ti<sup>3+</sup> and Ti<sup>4+</sup> expressed as TiO<sub>2</sub>

## Fluidization behaviour of various titania feedstocks

Table II  
Feedstock particle size distribution and density

Diameter range (µm)	Particle size distribution (wt %)					Density (g/cm <sup>3</sup> )				
	Slag A	Slag B	Slag C	Rutile	SR	Slag A	Slag B	Slag C	Rutile	SR
850	2.6	0.8	4.1			4.02	4.03	4.04	4.13	4.25
600–850	14.6	10.7	18.7							
425–600	19.6	13.7	19.8		0.9					
300–425	20.7	16.8	19.7		3.3					
212–300	17.1	15.6	15.2	2.0	16.5					
150–212	11.9	13.3	10.7	19.4	50.9	4.03	4.04	4.06	4.13	4.26
106–150	8.0	9.8	6.9	48.8	25.8	4.03	4.05	4.05	4.17	4.24
90–106	2.0	4.0	1.9	20.2	2.0	4.06	4.04	4.05	4.21	4.31
75–90	1.4	5.0	1.4	8.2	0.4	4.06	4.04	4.10	4.24	4.30
-75	2.1	10.2	1.6	1.3	0.2	4.10	4.06	4.10	4.25	4.30

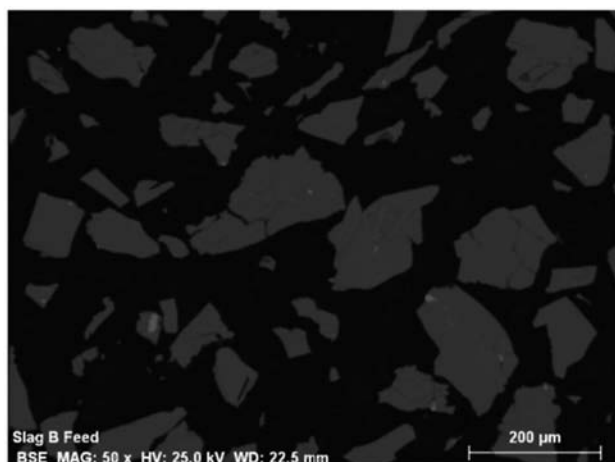


Figure 2—Backscattered electron image of a section through particles of Slag B

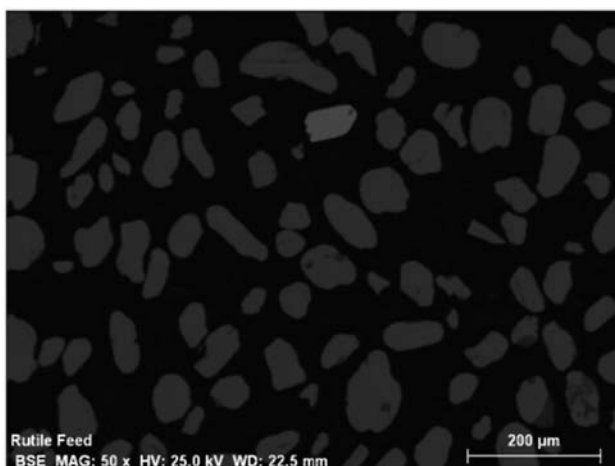


Figure 3—Backscattered electron image of a section through particles of rutile

Under ambient conditions, all feedstocks lie in Group B and are according to the Geldart classification, easy to fluidize. The larger fractions of the slags (i.e. >600 µm) belong to Group D.

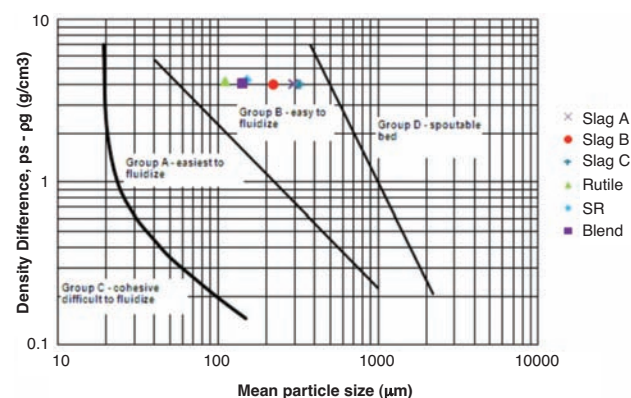


Figure 4—Geldart group classification

At operating temperatures and pressures above ambient, the material may appear in a different group from that which it occupies at ambient conditions, due to the change in gas properties.

### Fluidization properties

The velocity that marks the onset of fluidization is termed the minimum fluidizing velocity. This velocity can be estimated by Equation [3]<sup>1</sup>.

$$u_{mf} = \frac{(\phi_s d_p)^2}{150\mu} [g(\rho_s - \rho_g)] \frac{\epsilon_{mf}^3}{1 - \epsilon_{mf}} \quad [3]$$

The minimum fluidizing velocities for the feedstocks were calculated using the mean particle sizes (see Table III). The sphericity values for sharp sand and round sand from Kunii and Levenspiel<sup>1</sup> were used for the minimum fluidizing velocity calculation. Luckos and den Hoed<sup>3</sup> determined sphericity values for titania slag of between 0.439–0.555, which are slightly lower than the Kunii and Levenspiel<sup>1</sup> values. The density of air (at 1000°C) used was 0.27 kg/m<sup>3</sup>, while the viscosity of air (at 1000°C) used was 4.91×10<sup>-5</sup> kg/m.s.

The mean particle size of the slags is larger than the other feedstocks, and consequently the minimum fluidizing velocities are higher.

## Fluidization behaviour of various titania feedstocks

Table III

### Minimum fluidization velocities at 1000°C

Material	Density of solid (kg/m <sup>3</sup> )	Sphericity (from ref 1 for sand)	Voidage (from ref 1 for sand)	Mean particle size (µm)	Minimum fluidizing velocity at 1000°C (m/s)
Slag A	4030	0.67	0.50	294	0.05
Slag B	4040	0.67	0.50	218	0.03
Slag C	4050	0.67	0.49	322	0.06
Rutile	4190	0.86	0.48	110	0.01
SR	4260	0.86	0.44	151	0.02
Blend	4110	0.77	0.41	141	0.01

Terminal velocity ( $u_t$ ) for the various size fractions was calculated with Equations [4], [5], and [6]<sup>1</sup> (See Table IV). At gas velocities higher than the terminal velocity, particles will be blown out of the bed. Bubble size and disengagement height also play a role in determining which particles are entrained.

$$u_t = u^* \left( \frac{\mu(\rho_s - \rho_g)g}{\rho_g^2} \right)^{\frac{1}{3}} \quad [4]$$

$$u^* = \left[ \frac{18}{(d_p^*)^2} + \frac{2.335 - 1.744\phi_s}{(d_p^*)^{0.5}} \right]^{-1} \quad [5]$$

$$d_p^* = d_p \left[ \frac{\rho_g(\rho_s - \rho_g)g}{\mu^2} \right]^{\frac{1}{3}} \quad [6]$$

Most industrial chlorinators operate at a superficial velocity of 0.15 m/s, so particles with a terminal velocity lower than 0.15 m/s can be elutriated from the bed. In the trials, feedstocks were fluidized with a superficial velocity of 0.19 m/s. According to the calculated terminal velocity values, particles finer than 75 µm will be susceptible to elutriation since terminal velocity is lower than 0.19 m/s. Slag B has the highest fraction of particles less than 75 µm, and it is expected that about 10 per cent of Slag B will be elutriated compared to approximately 2 per cent of the other feedstocks.

### Elutriation constant

Figure 5 records the fraction blowover for each sample after the 30-minute fluidization experiment, and calculated elutriation constants are presented in Table V. The percentage blowover is calculated by Equation [7].

$$\text{Blowover (\%)} = \frac{M_E}{M_i} \times 100\% \quad [7]$$

Elutriation constants are proportional to the amount of material removed from a chlorinator. Smaller size fractions are more likely to be elutriated, and this is illustrated by the results. Elutriation constants for particles finer than 75 µm are more than three times greater than those for the adjacent, coarser size fraction. Blowovers from the rutile and SR sample are significantly lower than those of the slags. The finer material (i.e. <75 µm) had the highest tendency to be elutriated. A small fraction of the particles in 150–212 µm size range were also elutriated. Particles larger than 212 µm were not elutriated.

The slags have the highest blowovers and thus highest  $k_i^*$  values. Slag B had the highest mass of fines (i.e. particles < 75 µm) and thus blowover was the highest.

Table IV

### Terminal velocity of different feedstocks

Particle diameter (µm)	Terminal velocity (m/s)					
	Slag A	Slag B	Slag C	Rutile	SR	Blend
850	7.37	7.38	7.39			8.27
600	5.35	5.36	5.37		6.87	5.91
425	3.67	3.68	3.69		4.54	3.98
300	2.35	2.36	2.36	2.73	2.79	2.5
212	1.41	1.41	1.42	1.58	1.62	1.48
150	0.8	0.81	0.81	0.88	0.89	0.83
106	0.44	0.44	0.44	0.47	0.48	0.45
75	0.23	0.23	0.23	0.25	0.25	0.24
60	0.15	0.15	0.15	0.16	0.16	0.16
53	0.12	0.12	0.12	0.13	0.13	0.12

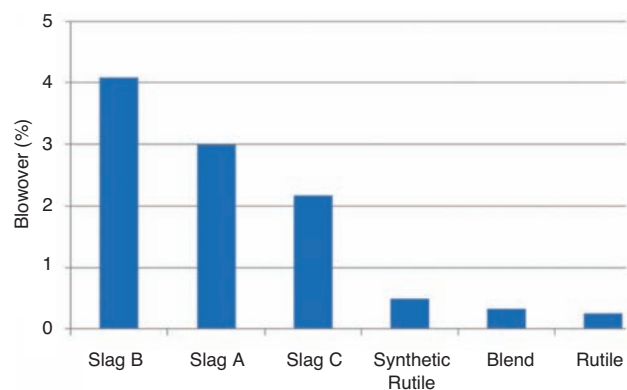


Figure 5—Blowover of each sample

Table V

### Elutriation constants

Diameter range	Elutriation constant ( $k_i^*$ ) > kg/m <sup>2</sup> s (x10 <sup>-3</sup> )					
	Slag A	Slag B	Slag C	Rutile	SR	Blend
150–212	0.30	0.30	0.23	0.02	0.05	0.00
106–150	2.50	2.40	2.10	0.04	0.37	0.03
75–106	7.00	2.80	4.50	0.08	1.70	0.11
<75	25.60	10.60	14.80	3.17	82.90	5.86

## Fluidization behaviour of various titania feedstocks

Chloride pigment producers do not usually feed the -106  $\mu\text{m}$  fraction to the chlorinator, but the results indicate that the fraction larger than 75  $\mu\text{m}$  and finer than 106  $\mu\text{m}$  does not pose as significant an elutriation problem as the fraction finer than 75  $\mu\text{m}$ .

The elutriation constants of the blend are lower than the average constants of rutile and Slag A. The values are closer to those of rutile, indicating that the blowover of slag is significantly reduced in the blend. It appears that the blending of two feedstocks changes the hydrodynamic behavior of the bed and results in lower blowover. With the combination of feedstocks, the bulk physical properties of the bed change. The most obvious is the change in particle size distribution and the mean particle size (i.e.  $d_{50}$ ). The  $d_{50}$  of Slag A is 294  $\mu\text{m}$  and the  $d_{50}$  of rutile is 110  $\mu\text{m}$ . By combining the feedstocks, we effectively widen the distribution.

Previous work<sup>4,5</sup> suggests that the gas bubble size is reduced when the bed is made up of particles with a wide particle size distribution. Sun and Grace<sup>5</sup> suggest the following as an explanation to why bubble size is reduced:

- The wider particle size distributions result in a more expanded dense phase, which in turn leads to more gas passing through the dense phase and to a reduced effective viscosity
- Associated with the lower effective dense-phase viscosity, voids or bubbles tend to be smaller with a wider particle size distribution.

Bubbles carry particles as they move through the bed, and when the bubble reaches the surface, it bursts and material is thrown into the freeboard area<sup>6-8</sup>. Smaller bubbles carry less material, which leads to lower entrainment rates. George and Grace<sup>9</sup> investigated the volume of ejected particles as a function of bubble size, and found that the volume of elutriated particles increases with increasing bubble size. Although it is unclear why the blowover from the blend is low compared to that of its individual components, the elutriation result has significant implications for slag and pigment producers. The results of this study show that if slag is fed together with rutile, the blowover can be lowered.

### Conclusion

A high elutriation rate translates to a shorter residence time for particles in the fluidized bed, which in turn lowers conversion efficiencies. Although the elutriation experiments were conducted in an inert environment, these results provide a comparative indication of the relative elutriation rates of feedstocks from a chlorinator. The blowovers from the three slags were higher than those of the rutile, SR, and the blend; this means that if the same amount of each feedstock is individually fed to a chlorinator, there will be more rutile and SR available for chlorination than slags. Particles finer than 212  $\mu\text{m}$  were elutriated, and particles finer than 75  $\mu\text{m}$  had the highest tendency to be elutriated.

The elutriation constants of the blend were lower than the average of its individual feedstocks. It is hypothesized that the wider particle size distribution of the blend leads to improved fluidization behaviour; however, further work is required to support this hypothesis. Nonetheless, the

elutriation results of the blend have significant implications for the slag and pigment producers. The results of this study show that if slag is fed together with rutile, the blowover can be lowered. It is recommended that chlorination tests are conducted on the individual feedstocks and blends to determine if the same trend is observed, and the implication for conversion rates.

### Acknowledgements

Exxaro is acknowledged for permission to publish this paper. Appreciation is also expressed to the reviewers for useful comments and insights on the paper.

### Notation

$d_p$	mean particle diameter, m
$d_p^*$	measure of particle diameter, dimensionless
$\rho_s$	density of solids, $\text{kg/m}^3$
$\rho_g$	density of gas, $\text{kg/m}^3$
$\Phi_s$	sphericity of particle, dimensionless
$\mu$	viscosity of gas, $\text{kg/m}\cdot\text{s}$
$\varepsilon_{mf}$	voidage at minimum fluidization, dimensionless
$u_t$	terminal velocity, m/s
$u^*$	measure of particle velocity, dimensionless
$u_{mf}$	minimum fluidizing velocity, m/s
$W_{i0}$	initial weight of mass fraction $i$ , g
$W_i$	final weight of mass fraction $i$ , g
$W$	total weight of sample before fluidization, g
$A$	cross-sectional area of reactor, $\text{m}^2$
$t$	time, s
$k_i^*$	elutriation constant, $\text{kg/m}^2\cdot\text{s}$
$M_E$	mass of material elutriated, g
$M_i$	initial sample mass, g
$x_i$	weight fraction of solids of size $i$ , dimensionless

### References

- KUNII, D. and LEVENSPIEL O. Fluidization Engineering. 2nd edn. Boston, Butterworth – Heineman, 1991.
- GELDART, D. Types of gas fluidization. *Powder Technology*, vol. 7, 1973. pp. 285–292.
- LUCKOS, A. and DEN HOED, P. Fluidization and flow regimes of titaniferous solids. *Industrial and Engineering Chemistry Research*, vol. 43, 2004. pp. 5645–5652.
- BEETSTRA, R., NIJENHUIS, J., ELLIS, N., and VAN OMMEN, J.R. The influence of particle size distribution on fluidized bed hydrodynamics using high through put experimentation. *AIChE Journal*, vol. 55, no. 8, 2009. pp. 2013–2023.
- GRACE, J.R. and SUN, G. 1991. Influence of particle size distribution on the performance of fluidized bed reactors. *Canadian Journal of Chemical Engineering*, vol. 69, 2009. pp. 1126–1134.
- SUN, G. and GRACE, J.R. The effect of particle size distribution on the performance of a catalytic fluidized bed reactor. *Chemical Engineering Science*, vol. 45, no. 8, 1990. pp. 2187–2194.
- BAEYENS, J., GELDART, D., and WU, S.Y. Elutriation of fines from gas fluidized beds of Geldart A type powders—effect of adding superfines. *Powder Technology*, vol. 71, 1992. pp. 71–80.
- WEN, C.Y. and CHEN, L.H. Fluidized bed freeboard phenomena: entrainment and elutriation. *AIChE Journal*, vol. 28, no. 1, 1982. pp. 117–128.
- GEORGE, S.E. and GRACE, J.R. Entrainment of particles from aggregative fluidized beds. *American Institute for Chemical Engineers, Symposium Series 74*, 1978. pp. 67–74. ◆